

The  $\text{Ag}_2\text{O}-\text{V}_2\text{O}_5-\text{HF}_{(\text{aq})}$  System and Crystal Structure of  $\alpha\text{-Ag}_3\text{VO}_4$ 

Thomas A. Albrecht, Charlotte L. Stern, and Kenneth R. Poeppelmeier\*

Department of Chemistry, Northwestern University, Evanston, Illinois 60208-3113

Received November 10, 2006

Reactions between the three components  $\text{Ag}_2\text{O}$ ,  $\text{V}_2\text{O}_5$ , and  $\text{HF}_{(\text{aq})}$  were investigated under hydrothermal conditions, and the recovered phases were, in increasing Ag:V content,  $\text{Ag}_2\text{V}_4\text{O}_{11}$ ,  $\beta\text{-AgVO}_3$ ,  $\text{Ag}_4\text{V}_2\text{O}_6\text{F}_2$ ,  $\text{Ag}_4\text{V}_2\text{O}_7$ , and  $\alpha\text{-Ag}_3\text{VO}_4$ . A higher ratio of  $\text{Ag}_2\text{O}$  to  $\text{V}_2\text{O}_5$ , as compared to a stoichiometric ratio, was required to synthesize  $\text{Ag}_4\text{V}_2\text{O}_6\text{F}_2$ ,  $\text{Ag}_4\text{V}_2\text{O}_7$ , and  $\alpha\text{-Ag}_3\text{VO}_4$ . Owing to their solubility differences, the crystallization regions are not centered around the respective 2:1 and 3:1  $\text{Ag}_2\text{O}/\text{V}_2\text{O}_5$  tie-lines but rather are centered along the 4:1 and 8:1  $\text{Ag}_2\text{O}/\text{V}_2\text{O}_5$  tie-lines. Reactions with a 4:1 Ag/V ratio either resulted in  $\text{Ag}_4\text{V}_2\text{O}_6\text{F}_2$  at 150 °C or  $\text{Ag}_4\text{V}_2\text{O}_7$  at 200 °C. Products were recovered in between 80% and 100% yield based on  $\text{V}_2\text{O}_5$ . Red transparent crystals of  $\alpha\text{-Ag}_3\text{VO}_4$  crystallize in the monoclinic space group  $C2/c$ , with cell parameters  $a = 10.1885(16)$  Å,  $b = 4.9751(8)$  Å,  $c = 10.2014(17)$  Å,  $\beta = 115.754(3)^\circ$ .

## Introduction

Mixed metal oxide fluoride species can be generated in direct hydrothermal reactions of early and late transition metal oxide precursors in the presence of hydrogen fluoride (e.g.,  $(\text{HF})_x$ -pyridine or  $\text{HF}_{(\text{aq})}$ ).<sup>1,2</sup> Whereas numerous inorganic–organic hybrid materials have been made, the use of  $\text{HF}_{(\text{aq})}$  has led to purely inorganic oxide fluorides, e.g.,  $\text{Ag}_6\text{Mo}_2\text{O}_7\text{F}_3\text{Cl}$  and  $\text{Ag}_4\text{V}_2\text{O}_6\text{F}_2$ .<sup>3–5</sup> In these reactions, aqueous HF acts as a mineralizer and provides a source of fluoride, which may be incorporated into the product.

Owing to their application as primary battery materials, the silver vanadium oxides have been studied intensely.<sup>6–8</sup> While various silver vanadates are known,  $\text{Ag}_4\text{V}_2\text{O}_6\text{F}_2$  represents the first phase reported in the  $\text{Ag}_2\text{O}-\text{V}_2\text{O}_5-\text{HF}_{(\text{aq})}$  system. This work focuses on the  $\text{Ag}_2\text{O}-\text{V}_2\text{O}_5-\text{HF}_{(\text{aq})}$

system to search for additional silver vanadium oxide fluoride phases and to elucidate the relationships between the other majority all-oxide phases formed. During this investigation, the well-known silver vanadium oxides  $\text{Ag}_2\text{V}_4\text{O}_{11}$ ,  $\beta\text{-AgVO}_3$ ,  $\text{Ag}_4\text{V}_2\text{O}_7$ , and  $\alpha\text{-Ag}_3\text{VO}_4$  were generated in addition to the aforementioned  $\text{Ag}_4\text{V}_2\text{O}_6\text{F}_2$ , of which only  $\text{Ag}_2\text{V}_4\text{O}_{11}$  and  $\beta\text{-AgVO}_3$  previously had been made hydrothermally.<sup>9,10</sup> The versatility of aqueous hydrofluoric acid to form a wide variety of silver vanadium oxides is noteworthy and appreciable compared to other techniques.

In the 1930's, Britton and Robinson more thoroughly investigated solutions of silver and vanadium salts first studied in the late 1800's.<sup>11</sup> Of interest were the ionic species remaining in the solutions upon precipitation of  $\text{AgVO}_3$ ,  $\text{Ag}_4\text{V}_2\text{O}_7$ , and  $\text{Ag}_3\text{VO}_4$ . For example, in solutions targeting a  $\text{Ag}_3\text{VO}_4$  precipitate, the ions present were not  $\text{Ag}^+$  and  $\text{VO}_4^{3-}$  but rather  $\text{Ag}^+$ ,  $\text{HVO}_4^{2-}$ , and  $\text{OH}^-$ . Konta et al. also studied solution chemistry of silver vanadium oxides by varying the pH between 7 and 14 and the temperature between 273 and 298 K, and various oxides such as  $\alpha\text{-AgVO}_3$ ,  $\beta\text{-AgVO}_3$ ,  $\text{Ag}_4\text{V}_2\text{O}_7$ , and  $\text{Ag}_3\text{VO}_4$  were synthesized from aqueous solutions of  $\text{AgNO}_3$  and either  $\text{NH}_4\text{VO}_3$  or  $\text{Na}_3\text{VO}_4$ .<sup>12</sup> Moreover, solid-state reactions between  $\text{Ag}_2\text{O}$  and  $\text{V}_2\text{O}_5$  have been used to form the aforementioned silver

\* To whom correspondence should be addressed. E-mail: krp@northwestern.edu.

- (1) Norquist, A. J.; Heier, K. R.; Stern, C. L.; Poeppelmeier, K. R. *Inorg. Chem.* **1998**, *37*, 6495–6501.
- (2) Norquist, A. J.; Heier, K. R.; Halasyamani, P. S.; Stern, C. L.; Poeppelmeier, K. R. *Inorg. Chem.* **2001**, *40*, 2015–2019.
- (3) Maggard, P. A.; Nault, T. S.; Stern, C. L.; Poeppelmeier, K. R. *J. Solid State Chem.* **2003**, *175*, 27–33.
- (4) Sorensen, E. M.; Izumi, H. K.; Vaughey, J. T.; Stern, C. L.; Poeppelmeier, K. R. *J. Am. Chem. Soc.* **2005**, *127*, 6347–6352.
- (5) Izumi, H. K.; Sorensen, E. M.; Vaughey, J. T.; Poeppelmeier, K. R. U.S. Provisional Patent 60,606,475, September 1, 2004.
- (6) Liang, C. C.; Bolster, M. E.; Murphy, R. M. U.S. Patent 4,310,609, January 12, 1982.
- (7) Liang, C. C.; Bolster, M. E.; Murphy, R. M. U.S. Patent 4,391,729, July 5, 1983.
- (8) Takeuchi, K. J.; Marschilok, A. C.; Davis, S. M.; Leising, R. A.; Takeuchi, E. S. *Coord. Chem. Rev.* **2001**, *219*, 283–310.

- (9) Mao, C.; Wu, X.; Pan, H.; Zhu, J.; Chen, H. *Nanotechnology* **2005**, *16*, 2892–2896.
- (10) Liu, Y.; Zhang, Y.; Hu, Y.; Qian, Y. *Chem. Lett.* **2005**, *34*, 146–147.
- (11) Britton, H. T. S.; Robinson, R. A. *J. Chem. Soc. Abstr.* **1930**, 2328–2343.
- (12) Konta, R.; Kato, H.; Kobayashi, H.; Kudo, A. *Phys. Chem. Chem. Phys.* **2003**, *5*, 3061–3065.

vanadates and two others, AgV<sub>7</sub>O<sub>18</sub> and Ag<sub>2</sub>V<sub>4</sub>O<sub>11</sub>.<sup>13</sup> Included in these reports were the transition temperatures between  $\alpha$ -,  $\beta$ -, and  $\gamma$ -AgVO<sub>3</sub> phases. Since then, crystal structures for Ag<sub>2</sub>V<sub>4</sub>O<sub>11</sub>,  $\alpha$ - and  $\beta$ -AgVO<sub>3</sub>, and Ag<sub>4</sub>V<sub>2</sub>O<sub>7</sub> have been solved and phases such as  $\delta$ -AgVO<sub>3</sub>,  $\beta$ -Ag<sub>3</sub>VO<sub>4</sub>, and nonstoichiometric compounds, such as Ag<sub>x</sub>V<sub>2</sub>O<sub>5</sub> and Ag<sub>1+x</sub>V<sub>3</sub>O<sub>8</sub>, have been observed.<sup>14–18</sup> During review of this manuscript, the authors became aware of an independent study on the structures of  $\alpha$ - and  $\beta$ -Ag<sub>3</sub>VO<sub>4</sub> from refinement of powder X-ray diffraction patterns.<sup>19</sup>

Recently, other processes have been reported to synthesize silver vanadium oxides. For example, sol–gel techniques have been used for the synthesis of Ag<sub>2</sub>V<sub>4</sub>O<sub>11</sub>. The process involves a V<sub>2</sub>O<sub>5</sub>·*n*H<sub>2</sub>O gel combined with a silver-containing salt, which is then heated at up to 450 °C for up to 24 h. Another method investigated by Kittaka et al. utilized mechanical ball milling of different ratios of Ag<sub>2</sub>O and V<sub>2</sub>O<sub>5</sub> to produce amorphous  $\alpha$ -AgVO<sub>3</sub>, crystalline Ag<sub>4</sub>V<sub>2</sub>O<sub>7</sub>, or Ag<sub>3</sub>VO<sub>4</sub> with additional phases.<sup>20</sup>

Very few reports exist in the literature discussing the synthesis of silver vanadium oxides using hydrothermal techniques. Liu et al. produced small microcrystals 18–400 nm wide and lengths of up to tens of micrometers (nanowires) of  $\beta$ -AgVO<sub>3</sub> from solutions of NH<sub>4</sub>VO<sub>3</sub> and either Ag<sub>2</sub>CO<sub>3</sub> or AgC<sub>2</sub>H<sub>3</sub>O<sub>2</sub> heated under hydrothermal conditions.<sup>10</sup> Additional phases were also recovered, such as  $\alpha$ -AgVO<sub>3</sub>, upon variation of temperature, pH, and reagents. Takeuchi et al. proposed the use of hydrothermal methods in the synthesis of the cathode material Ag<sub>2</sub>V<sub>4</sub>O<sub>11</sub> (SVO).<sup>21</sup> The desired small particle size (<1  $\mu$ m in diameter) has potential to improve the modern high-rate SVO batteries by providing higher current pulses more rapidly. Experimental details remain to be specified. However, Mao et al. synthesized 10–30 nm thick, 70–200 nm wide, and 2–5 mm long crystallites (nanobelts) of Ag<sub>2</sub>V<sub>4</sub>O<sub>11</sub> from an aqueous solution of V<sub>2</sub>O<sub>5</sub>, AgNO<sub>3</sub>, and 1,6-hexanediamine heated under hydrothermal conditions at 180 °C for 2 days.<sup>9</sup>

From the hydrothermal reactions and conditions reported herein, four silver vanadium oxides and one silver vanadium oxide fluoride were observed. Polycrystalline Ag<sub>2</sub>V<sub>4</sub>O<sub>11</sub> and  $\beta$ -AgVO<sub>3</sub> and single crystals of Ag<sub>4</sub>V<sub>2</sub>O<sub>6</sub>F<sub>2</sub>, Ag<sub>4</sub>V<sub>2</sub>O<sub>7</sub>, and  $\alpha$ -Ag<sub>3</sub>VO<sub>4</sub>—the structure of the latter is reported here also—were synthesized by reaction of the binary oxides Ag<sub>2</sub>O and V<sub>2</sub>O<sub>5</sub> with HF<sub>(aq)</sub> as a mineralizer in a pressure vessel at 150–200 °C under autogenous pressure. The composition space

**Table 1.** Crystallographic Data for Ag<sub>3</sub>VO<sub>4</sub>

formula	Ag <sub>3</sub> VO <sub>4</sub>
fw	438.55
space group	C2/c (No. 15)
<i>a</i> (Å)	10.1885(16)
<i>b</i> (Å)	4.9751(8)
<i>c</i> (Å)	10.2014(17)
$\beta$ (deg)	115.754(3)
<i>V</i> (Å <sup>3</sup> )	465.73(13)
<i>Z</i>	4
<i>T</i> (°C)	–120(2)
$\lambda$ (Å)	0.71069
$\sigma_{\text{calcd}}$ (g/cm <sup>3</sup> )	6.254
$\mu$ (mm <sup>–1</sup> )	14.266
R1( <i>F</i> ) <sup>a</sup>	0.0295
wR2( <i>F</i> <sup>2</sup> ) <sup>b</sup>	0.0771

$$^a \text{R1} = \sum |F_o| - |F_c| / \sum |F_o|, \quad ^b \text{wR2} = [\sum w(F_o^2 - F_c^2)^2 / \sum w(F_o^2)]^{1/2}.$$

for Ag<sub>2</sub>O–V<sub>2</sub>O<sub>5</sub>–HF<sub>(aq)</sub> was constructed by varying the molar ratio of reagents while maintaining a constant total number of moles. Regions in the composition space diagram are outlined on the basis of the identity of the recovered products as determined by powder X-ray diffraction. Though a mixture of products is recovered from reactions when a composition lies on or near a boundary between regions, single phases were formed in the middle of a defined region.

## Experimental Section

**Caution.** Hydrofluoric acid is toxic and corrosive and must be handled with extreme caution and the appropriate protective gear! If contact with the liquid or vapor occurs, proper treatment procedures should be followed immediately.<sup>22–24</sup>

**Materials.** Ag<sub>2</sub>O (99.5%, DFG), V<sub>2</sub>O<sub>5</sub> (99.6%, Alfa-Aesar), and aqueous hydrofluoric acid (48–50% HF by weight, Fisher) were used as received.

**Synthesis.** Crystals of  $\alpha$ -Ag<sub>3</sub>VO<sub>4</sub> were prepared from a reaction of 0.5675 g (2.449  $\times$  10<sup>–3</sup> mol) of Ag<sub>2</sub>O, 0.0557 g (3.06  $\times$  10<sup>–4</sup> mol) of V<sub>2</sub>O<sub>5</sub>, and 0.2522 g of HF<sub>(aq)</sub> (6.179  $\times$  10<sup>–3</sup> mol HF) in a heat-sealed Teflon [fluoro(ethylene–propylene)] pouch.<sup>25</sup> The pouch was placed in a 125 mL, poly(tetrafluoroethylene) (PTFE) Teflon-lined Parr autoclave, backfilled with 42 mL of deionized H<sub>2</sub>O. Up to seven pouches of varied compositions were simultaneously placed in the autoclave to complete a greater quantity of reactions while using one pressure vessel. The autoclave was heated at 150 °C for 24 h and cooled at a rate of 6 °C/h. The pouch was opened in air, and the contents were vacuum-filtered to retrieve bright red crystals of  $\alpha$ -Ag<sub>3</sub>VO<sub>4</sub> in 78% yield based on V<sub>2</sub>O<sub>5</sub>. Identical reaction conditions, other than reagent ratios, were used to make Ag<sub>2</sub>V<sub>4</sub>O<sub>11</sub>,  $\beta$ -AgVO<sub>3</sub>, and Ag<sub>4</sub>V<sub>2</sub>O<sub>6</sub>F<sub>2</sub>. Products were analyzed by powder X-ray diffraction.

Ag<sub>2</sub>V<sub>4</sub>O<sub>11</sub> was made using 0.2678 g (1.155  $\times$  10<sup>–3</sup> mol) of Ag<sub>2</sub>O, 0.4198 g (2.308  $\times$  10<sup>–3</sup> mol) of V<sub>2</sub>O<sub>5</sub>, and 0.2328 g of HF<sub>(aq)</sub> (5.703  $\times$  10<sup>–3</sup> mol HF). The product was recovered in 98% yield based on V<sub>2</sub>O<sub>5</sub> with a trace of  $\beta$ -AgVO<sub>3</sub>.

$\beta$ -AgVO<sub>3</sub> was made from 0.2979 g (1.285  $\times$  10<sup>–3</sup> mol) of Ag<sub>2</sub>O, 0.1559 g (8.571  $\times$  10<sup>–4</sup> mol) of V<sub>2</sub>O<sub>5</sub>, and 0.2572 g of HF<sub>(aq)</sub> (6.301  $\times$  10<sup>–3</sup> mol HF) with 80% recovery based on V<sub>2</sub>O<sub>5</sub>.

Ag<sub>4</sub>V<sub>2</sub>O<sub>6</sub>F<sub>2</sub> was made as previously reported.<sup>5</sup>

- (13) Fleury, P.; Kohlmuller, R. C. *R. Acad. Sci. Ser. C* **1966**, 262, 475–477.
- (14) Kittaka, S.; Matsuno, K.; Akashi, H. *J. Solid State Chem.* **1999**, 142, 360–367.
- (15) Rozier, P.; Savariault, J.-M.; Galy, J. J. *J. Solid State Chem.* **1996**, 122, 303–308.
- (16) Masse, R.; Averbuch-Pouchot, M. T.; Durif, A.; Guitel, C. *Acta Crystallogr., Sect. C: Cryst. Struct. Commun.* **1983**, 39, 1608–1610.
- (17) Onoda, M.; Kanbe, K. *J. Phys.: Condens. Matter* **2001**, 13, 6675–6685.
- (18) Raveau, B. *Rev. Chim. Miner.* **1967**, 4, 729–758.
- (19) Kovalevskij, A.; Dinnebier, R.; Jansen, M. *Z. Krist.* **2007**, in press.
- (20) Kittaka, S.; Nishida, S.; Ohtani, T. *J. Solid State Chem.* **2002**, 169, 139–142.
- (21) Takeuchi, E. S.; Leising, R.; Rubino, R.; Hong, G. U.S. Provisional Patent 20,040,185,346, March 19, 2004.

- (22) Bertolini, J. C. *J. Emerg. Med.* **1992**, 10, 163–168.
- (23) Segal, E. B. *Chem. Health Saf.* **2000**, 7, 18–23.
- (24) Peters, D.; Miethchen, R. *J. Fluorine Chem.* **1996**, 79, 161–165.
- (25) Harrison, W. T. A.; Nenoff, T. M.; Gier, T. E.; Stucky, G. D. *Inorg. Chem.* **1993**, 32, 2437–2441.

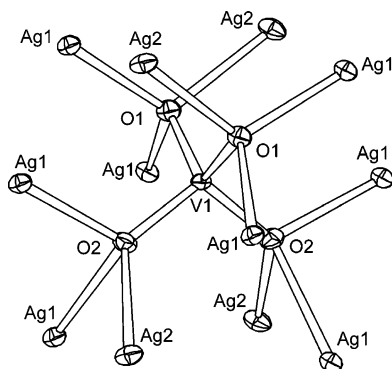


**Figure 1.** Thermal ellipsoid plot (showing 50% probability) of  $\alpha$ - $\text{Ag}_3\text{VO}_4$ . Vanadium is tetrahedrally coordinated to four oxide ions. Each oxide ion is tetrahedrally coordinated to one vanadium and three silver ions.

$\text{Ag}_4\text{V}_2\text{O}_7$  was made using 0.3970 g ( $1.713 \times 10^{-3}$  mol) of  $\text{Ag}_2\text{O}$ , 0.0777 g ( $4.272 \times 10^{-4}$  mol) of  $\text{V}_2\text{O}_5$ , and 0.2561 g of  $\text{HF}_{(\text{aq})}$  ( $6.274 \times 10^{-3}$  mol HF). However, the system was heated for 24 h at 200 °C instead of 150 °C. The product was recovered in 100% yield based on  $\text{V}_2\text{O}_5$ .

**Crystallographic Determination.** Single-crystal X-ray diffraction data were collected on a Bruker SMART-1000 diffractometer equipped with Mo K $\alpha$  radiation ( $\lambda = 0.71073$  Å). Reflections were integrated with the SAINT-Plus program.<sup>26</sup> The structure was solved in space group of  $C2/c$  by direct methods and refined against  $F^2$  using full-matrix least-squares techniques.<sup>27</sup> The  $\alpha$ - $\text{Ag}_3\text{VO}_4$  crystal was twinned, and absorption correction on one twinned data set was applied using Twinabs, a part of the SAINT integration program. That set of diffraction points was used to solve the structure including anisotropic displacement parameters before a final refinement with all reflections. See Table 1 for crystallographic data, Figure 1 for a thermal ellipsoid plot, and the Supporting Information for the crystallographic information file.

**Powder X-ray Diffraction.** Powder X-ray diffraction patterns were collected on a Rigaku XDS 2000 with Ni-filtered Cu K $\alpha$  radiation ( $\lambda = 1.5418$  Å) and compared with patterns recorded in the JCPDS (Joint Committee of Powder Diffraction Standards) database.

## Results and Discussion

At different mole ratios of  $\text{Ag}_2\text{O}$ ,  $\text{V}_2\text{O}_5$ , and  $\text{HF}_{(\text{aq})}$  in the hydrothermal system at 150 °C,  $\text{Ag}_2\text{V}_4\text{O}_{11}$ ,  $\beta$ - $\text{AgVO}_3$ ,  $\text{Ag}_4\text{V}_2\text{O}_6\text{F}_2$ , and  $\alpha$ - $\text{Ag}_3\text{VO}_4$  are observed (Figure 2). Unlike the solid-state reaction products,  $\text{AgV}_7\text{O}_{18}$  and  $\text{Ag}_4\text{V}_2\text{O}_7$  were not observed.<sup>13</sup> Particularly noteworthy is the presence of a single oxyfluoride  $\text{Ag}_4\text{V}_2\text{O}_6\text{F}_2$  and the absence of the oxide  $\text{Ag}_4\text{V}_2\text{O}_7$  (at 150 °C), both which have the same Ag/V ratio. However, at 200 °C,  $\text{Ag}_4\text{V}_2\text{O}_7$  is observed instead of  $\text{Ag}_4\text{V}_2\text{O}_6\text{F}_2$ , which will be addressed later. The composition space focused on the  $\text{HF}_{(\text{aq})}$ -rich region because experiments with insufficient  $\text{HF}_{(\text{aq})}$  under any of the aforementioned conditions resulted in incomplete solubilization and only partial reaction of the reactants. In addition, in order to optimize the synthesis (in particular the yield) of  $\text{Ag}_4\text{V}_2\text{O}_6\text{F}_2$ , the composition space diagram was studied in two different ways. First, varying the  $\text{Ag}_2\text{O}/\text{V}_2\text{O}_5$  ratio while maintaining

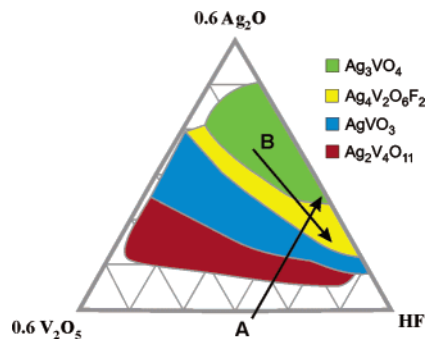


**Figure 2.** Composition space for the hydrothermal system of  $\text{Ag}_2\text{O}-\text{V}_2\text{O}_5-\text{HF}_{(\text{aq})}$ . Formation regions for the silver vanadates and the silver vanadium oxide fluoride are outlined. Line A represents a constant  $\text{HF}_{(\text{aq})}$  quantity while varying  $\text{Ag}_2\text{O}/\text{V}_2\text{O}_5$  ratio, increasing toward a higher silver fraction. Line B represents a constant 4:1  $\text{Ag}_2\text{O}/\text{V}_2\text{O}_5$  ratio, increasing toward a higher  $\text{HF}_{(\text{aq})}$  fraction.

**Table 2.** Products of the Hydrothermal  $\text{Ag}_2\text{O}-\text{V}_2\text{O}_5-\text{HF}_{(\text{aq})}$  System Are Dependent on the Molar Concentration of  $\text{HF}_{(\text{aq})}$  at Varying Ag:V Ratios<sup>a</sup>

Ag/V/ $\text{HF}_{(\text{aq})}$	x			
	$\text{Ag}_2\text{V}_4\text{O}_{11}$	$\text{AgVO}_3$	$\text{Ag}_4\text{V}_2\text{O}_6\text{F}_2$	$\text{Ag}_3\text{VO}_4$
1:1:x	8	4		
2:1:x		15	7	
4:1:x			15	4
8:1:x				20

<sup>a</sup> It should be noted that the values for x are not accounting for the moles of water in  $\text{HF}_{(\text{aq})}$ .

a constant overall metal oxide/ $\text{HF}_{(\text{aq})}$  ratio (Figure 2, Line A), and second, keeping the  $\text{Ag}_2\text{O}/\text{V}_2\text{O}_5$  ratio fixed while varying the amount of  $\text{HF}_{(\text{aq})}$  in the system (Figure 2, Line B).

**Constant  $\text{HF}_{(\text{aq})}$ .** In the first trend, reactions with an increasing  $\text{Ag}_2\text{O}/\text{V}_2\text{O}_5$  ratio yield products with higher silver contents. However, there is no direct stoichiometric relationship between the  $\text{Ag}_2\text{O}/\text{V}_2\text{O}_5$  starting ratio and the silver-to-vanadium ratio in the product. For example, 1:1  $\text{Ag}_2\text{O}/\text{V}_2\text{O}_5$  in a hydrothermal reaction (this work), in a typical solid-state reaction, or in a mechanochemical reaction yields  $\beta$ - $\text{AgVO}_3$ .<sup>13,20,28</sup> However, at 2:1  $\text{Ag}_2\text{O}/\text{V}_2\text{O}_5$  the reported system (with an appropriate quantity of  $\text{HF}_{(\text{aq})}$ , mentioned later) yields  $\beta$ - $\text{AgVO}_3$ , whereas in solid state and mechanochemical reactions  $\text{Ag}_4\text{V}_2\text{O}_7$  forms. For hydrothermal reactions,  $\text{Ag}_4\text{V}_2\text{O}_6\text{F}_2$  is phase pure at 4:1  $\text{Ag}_2\text{O}/\text{V}_2\text{O}_5$ , and similarly  $\alpha$ - $\text{Ag}_3\text{VO}_4$  is only obtained phase-pure at ratios of 8:1  $\text{Ag}_2\text{O}/\text{V}_2\text{O}_5$ . The silver not incorporated in the final solid product for the reported system remains in solution, rather than forming an amorphous phase, as evidenced by precipitation of  $\text{AgCl}$  with hydrochloric acid. Other hydrothermal syntheses of silver-containing compounds have also been more successful (higher yield) upon an excess addition of the silver-containing reagent.<sup>29,30</sup> Indeed, as early as 1930, it was noted that precipitation of  $\text{Ag}_3\text{VO}_4$  from 3:1 sodium vanadate and  $\text{AgNO}_3$  occurred more readily with excess  $\text{AgNO}_3$ .<sup>11</sup>

(26) SAINT-Plus, version 6.02A; Bruker Analytical X-ray Instruments, Inc.: Madison, WI, 2000.

(27) Sheldrick, G. M. SHELXTL, version 5.10; Bruker Analytical X-Ray Instruments, Inc.: Madison, WI, 1997.

(28) Kittaka, S.; Nishida, S.; Iwashita, T.; Ohtani, T. *J. Solid State Chem.* **2002**, *164*, 144–149.

(29) Barthelet, K.; Riou, D.; Ferey, G. *Solid State Sci.* **2001**, *3*, 203–209.

(30) Hu, J. Q.; Deng, B.; Zhang, W. X.; Tang, K. B.; Qian, Y. T. *Int. J. Inorg. Mater.* **2001**, *3*, 639–642.

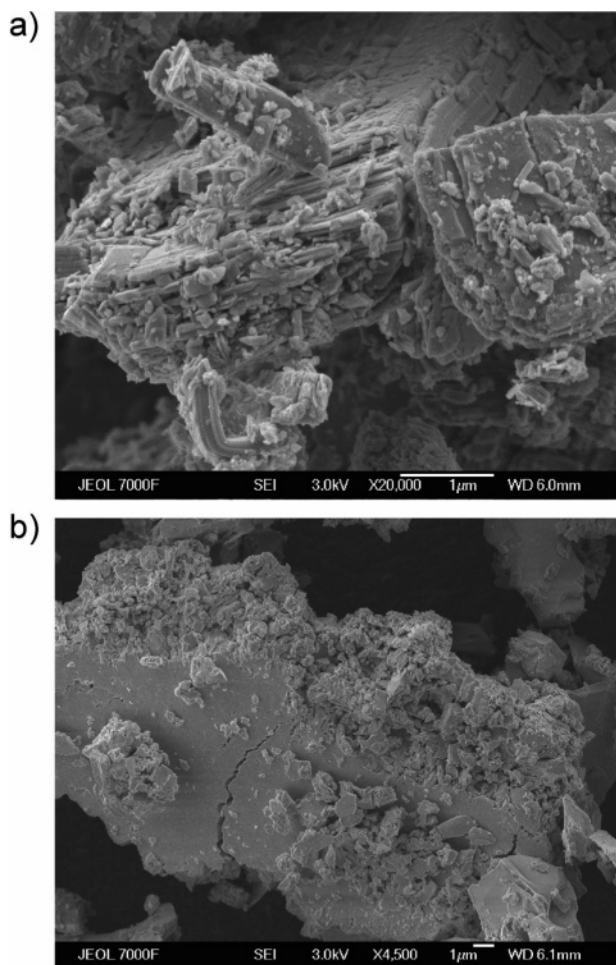


**Figure 3.** SEM of (a)  $\text{Ag}_2\text{V}_4\text{O}_{11}$  and (b)  $\text{Ag}_4\text{V}_2\text{O}_6\text{F}_2$  particles from hydrothermal synthesis.

**Constant  $\text{Ag}_2\text{O}/\text{V}_2\text{O}_5$ .** The second trend in the  $\text{Ag}_2\text{O}-\text{V}_2\text{O}_5-\text{HF}_{(\text{aq})}$  composition space shows that product formation depends on the quantity of  $\text{HF}_{(\text{aq})}$  added, while maintaining a constant  $\text{Ag}_2\text{O}/\text{V}_2\text{O}_5$  ratio. The mineralizer in the hydrothermal reactions plays an important role in determining the speciation and solubilities of reactants. Reactions are more favorable when the mineralizer initially helps solubilize the reactants, but if the mineralizer prevents any product from forming by either dissolving it or stabilizing the reactant species in solution, no reaction occurs.<sup>31</sup> In the aforementioned system, the higher mole ratio of  $\text{HF}_{(\text{aq})}$  solubilizes some of the silver well enough to prevent it from combining with vanadium into a precipitate (Table 2). At a 1:1  $\text{Ag}_2\text{O}/\text{V}_2\text{O}_5$  ratio,  $\beta\text{-AgVO}_3$  was obtained at a low  $\text{HF}_{(\text{aq})}$  quantity and  $\text{Ag}_2\text{V}_4\text{O}_{11}$  was made by increasing the  $\text{HF}_{(\text{aq})}$  content. At a 2:1  $\text{Ag}_2\text{O}/\text{V}_2\text{O}_5$  ratio,  $\text{Ag}_4\text{V}_2\text{O}_6\text{F}_2$  formed with a low  $\text{HF}_{(\text{aq})}$  concentration, and increasing the  $\text{HF}_{(\text{aq})}$  quantity yielded  $\text{AgVO}_3$ . Finally, at a 4:1  $\text{Ag}_2\text{O}/\text{V}_2\text{O}_5$  ratio,  $\alpha\text{-Ag}_3\text{VO}_4$  formed with a low  $\text{HF}_{(\text{aq})}$  concentration while  $\text{Ag}_4\text{V}_2\text{O}_6\text{F}_2$  formed at a higher  $\text{HF}_{(\text{aq})}$  concentration.

The two tendencies above, however, do not address completely the formation of  $\text{Ag}_4\text{V}_2\text{O}_7$  in lieu of  $\text{Ag}_4\text{V}_2\text{O}_6\text{F}_2$

(31) Sheets, W. C.; Mugnier, E.; Barnabe, A.; Marks, T. J.; Poeppelmeier, K. R. *Chem. Mater.* **2006**, *18*, 7–20.

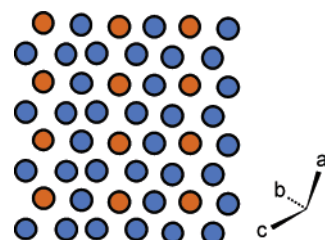


**Figure 4.** Close-packed layer in  $\alpha\text{-Ag}_3\text{VO}_4$ . Blue = Ag, orange = V.

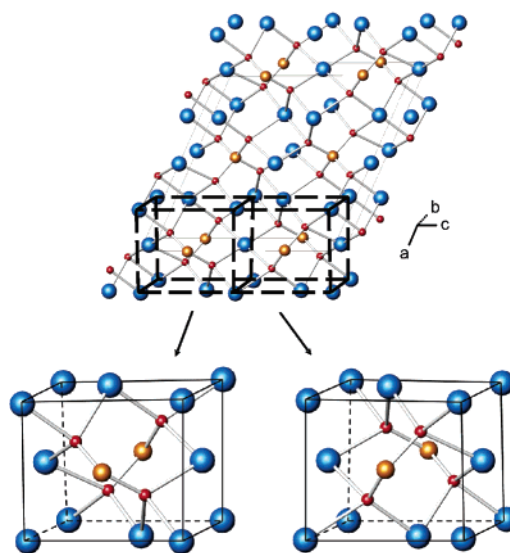


**Figure 5.** Primitive cells in  $\alpha\text{-Ag}_3\text{VO}_4$  have a distorted “anti” sphalerite-type structure of face-centered Ag and V cations with  $\text{O}^{2-}$  anions in either  $T_+$  or  $T_-$  holes. Blue = Ag, orange = V, red = O.

in the composition space. Originally with the intent of growing larger crystals of  $\text{Ag}_4\text{V}_2\text{O}_6\text{F}_2$ , hydrothermal reactions were carried out at higher temperatures (200 °C) where larger, red-orange crystals of  $\text{Ag}_4\text{V}_2\text{O}_7$  were recovered. To study the differences between the two systems producing  $\text{Ag}_4\text{V}_2\text{O}_6\text{F}_2$  and  $\text{Ag}_4\text{V}_2\text{O}_7$ , a series of reactions was performed using alternate heating temperatures and durations (equal amounts of reactants were loaded into the reaction pouches to form the two different products). Similar heating profiles were used, as described previously, with holding the maximum temperature between 150 and 200 °C at 10 °C increments. Whereas  $\text{Ag}_4\text{V}_2\text{O}_7$  was observed at temperatures as low as 170 °C, it was the dominant phase replacing  $\text{Ag}_4\text{V}_2\text{O}_6\text{F}_2$  above 190 °C. The silver vanadium oxide phases observed from reactions at 150 °C were also observed from reactions at 200 °C. Because reactions heated to a maximum temperature of 200 °C were cooled slowly, such reactions would be at temperature above 150 °C for 500 min longer than those where the maximum temperature was initially 150 °C. Adjustments to the heating duration such that the total reaction time (heating and cooling) were the same at any given maximum temperature yielded no difference.

In regard to the earlier discussion on small particle sizes of the battery material  $\text{Ag}_2\text{V}_4\text{O}_{11}$ , the particle sizes the battery materials made in the reported system were considered. Synthesis of  $\text{Ag}_2\text{V}_4\text{O}_{11}$  yielded particles that are on the order

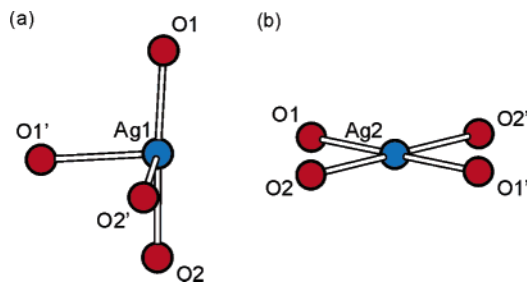


**Figure 6.** Coordination environment of silver atoms in  $\alpha$ - $\text{Ag}_3\text{VO}_4$ . (a) Pseudo-see-saw with bond angles of  $\text{O1-Ag1-O1}' = 98.13(9)^\circ$ ,  $\text{O1-Ag1-O2}' = 100.73(14)^\circ$ ,  $\text{O1-Ag1-O2} = 176.47(15)^\circ$ ,  $\text{O1}'\text{-Ag1-O2}' = 91.11(13)^\circ$ ,  $\text{O1}'\text{-Ag1-O2} = 84.40(13)^\circ$ , and  $\text{O2}'\text{-Ag1-O2} = 81.54(14)^\circ$  and bond lengths  $\text{Ag1-O1} = 2.164(4) \text{ \AA}$ ,  $\text{Ag1-O1}' = 2.444(4) \text{ \AA}$ ,  $\text{Ag1-O2} = 2.505(4) \text{ \AA}$ , and  $\text{Ag1-O2}' = 2.196(4) \text{ \AA}$ . (b) Distorted square planer with linear  $\text{O1-Ag2-O1}$  and  $\text{O2-Ag2-O2}$  bond angles and  $\text{O1-Ag2-O2} = 97.57(14)^\circ$  and bond lengths  $\text{Ag2-O1/O1}' = 2.364(4) \text{ \AA}$  and  $\text{Ag2-O2/O2}' = 2.374(4) \text{ \AA}$ .

of  $1 \mu\text{m}$  in dimensions (Figure 3a).<sup>32</sup> In contrast, the particle sizes of as-prepared  $\text{Ag}_4\text{V}_2\text{O}_6\text{F}_2$  are more widely dispersed from large crystals to sub-micrometer particles (Figure 3b). Synthesis of more uniformly small sized particles may also improve the performance of batteries incorporating  $\text{Ag}_4\text{V}_2\text{O}_6\text{F}_2$  as the active cathode material.

**Structure of  $\alpha$ - $\text{Ag}_3\text{VO}_4$ .** The structure of  $\alpha$ - $\text{Ag}_3\text{VO}_4$  consists of a cubic close-packed arrangement of metal ions (silver and vanadium) with the oxide anions occupying half of the tetrahedral positions, roughly creating an “anti” sphalerite-type (ZnS) structure (Figure 4). However, sphalerite-type does not adequately describe the extended structure for a number of reasons. First, the cations occupy the close-packed positions rather than anions (ergo the “anti” modifier). Second, the oxide anions are split between  $T_+$  and  $T_-$  holes (Figure 5), which also changes the coordination around the cations, in this case, only around silver, while vanadium is tetrahedrally coordinated to four oxide ligands. The presence of isolated  $[\text{VO}_4]^{3-}$  tetrahedra had been demonstrated previously by infrared and Raman studies.<sup>33</sup> The  $[\text{VO}_4]^{3-}$  anion has bond lengths of  $\text{V-O1} = 1.732(4) \text{ \AA}$  and  $\text{V-O2} = 1.711(4) \text{ \AA}$  and bond angles of  $\text{O1-V-O1} = 110.5(3)^\circ$ ,  $\text{O1-V-O2} = 110.95(18)^\circ$  and  $108.18(18)^\circ$ , and  $\text{O2-V-O2} = 108.0(3)^\circ$ . Silver in  $\alpha$ - $\text{Ag}_3\text{VO}_4$  has two different coordination spheres (Figure 6). With four oxide ligands, silver is either distorted square planar with  $D_{2h}$  symmetry or in a pseudo-see-saw arrangement with  $C$  symmetry. The volume around silver beyond the oxygen coordination sphere includes more silver at distances of  $2.9619(9) \text{ \AA}$ ,  $3.1771(6) \text{ \AA}$ , and  $3.2190(6) \text{ \AA}$ . Silver-silver distances less than  $3.0 \text{ \AA}$  are common to a few solid-state compounds, including silver pyrovanadate,  $\text{Ag}_4\text{V}_2\text{O}_7$ , which has minimum silver distances of  $2.989 \text{ \AA}$ .<sup>16,34</sup> Characteristics such as a sharp absorption

edge in the UV-visible light spectrum and electrical and ionic conductivity are common to materials with  $d^{10}$  silver cations. Indeed,  $\alpha$ - $\text{Ag}_3\text{VO}_4$  is bright red and was reported to increase the ionic conductivity of silver at ambient temperature when added to either  $\text{CuI}$  or  $\text{AgI}$ .<sup>35,36</sup>

$\text{K}_3\text{VO}_4$  and  $\text{K}_3\text{Cr}(\text{O}_2)_4$  are two compounds with structures similar to that of  $\alpha$ - $\text{Ag}_3\text{VO}_4$ .<sup>37,38</sup> Both structures are “anti” sphalerite-type with cations in a cubic close-packed arrangement and the oxide or peroxide anions, unlike  $\alpha$ - $\text{Ag}_3\text{VO}_4$ , occupy in only the  $T_+$  holes. The reason why  $\alpha$ - $\text{Ag}_3\text{VO}_4$  exhibits alternating cells of opposite tetrahedral positions may be because of the interactions between silver ions. Jansen notes that there are frequently drastic differences between structures of ternary silver(I) oxides and their sodium or potassium analogues, where the monovalent cation is present in a high ratio, such as the tendency for the silver cations to aggregate to form two-dimensional ribbons or layers with the silver-silver distances less than  $3.30 \text{ \AA}$ .<sup>34</sup>

## Conclusions

The  $\text{Ag}_2\text{O-V}_2\text{O}_5\text{-HF}_{(\text{aq})}$  system produces a variety of silver vanadium oxides and one silver vanadium oxide fluoride under the hydrothermal conditions at  $150 \text{ }^\circ\text{C}$ . Elevating the temperature,  $\text{Ag}_4\text{V}_2\text{O}_7$  is formed instead of  $\text{Ag}_4\text{V}_2\text{O}_6\text{F}_2$  at  $200 \text{ }^\circ\text{C}$ . The versatility of this system was shown in producing four stoichiometrically different silver vanadium oxides, as well as forming particles of  $\text{Ag}_2\text{V}_4\text{O}_{11}$  potentially small enough for improving specific applications and excellent crystals of  $\alpha$ - $\text{Ag}_3\text{VO}_4$  large enough for the single-crystal X-ray diffraction study.

**Acknowledgment.** The authors gratefully acknowledge the support from the National Science Foundation (Solid-State Chemistry Awards No. DMR-0312136 and DMR-0604454) and the use of the Central Facilities supported by the MRSEC program of the National Science Foundation (DMR-0076097 and DMR-0520513) at the Materials Research Center of Northwestern University.

**Supporting Information Available:** An X-ray crystallographic file in CIF format including crystallographic details, atomic coordinates, anisotropic thermal parameters, interatomic distances, and angles. This material is available free of charge via the Internet at <http://pubs.acs.org>.

IC062138+

(32) Bertoni, M. I.; Kidner, N. J.; Mason, T. O.; Albrecht, T. A.; Sorensen, E. M.; Poepplmeier, K. R. *J. Electroceram.* **2006**, submitted.

(33) Kristallov, L. V.; Volkov, V. L.; Perelyaeva, L. A. *Zh. Neorg. Khim.* **1990**, *35*, 1810–1814.

(34) Jansen, M. *Angew. Chem.* **1987**, *99*, 1136–1149.

(35) Viswanathan, A.; Suthanthiraraj, S. A. In *Solid State Ionics: New Developments, [Proceedings of the Asian Conference], 5th*; Kandy, Sri Lanka, Dec. 2–7, 1996; Chowdari, B. V. R.; Dissanayake, M. A. K. L.; Careem, M. A. Eds.; World Scientific: Singapore, 1996.

(36) Mishchenko, A. V.; Krasnova, T. M.; Yaufman, A. P. *J. Electroceram.* **1979**, *3*, 92–93.

(37) Olazcuaga, R.; Reau, J. M.; LeFlem, G.; Hagenmuller, P. *Z. Anorg. Allg. Chem.* **1975**, *412*, 271–280.

(38) Stomberg, R. *Acta Chem. Scand.* **1963**, *17*, 1563–1566.